SIGNAL INJECTION BASED FAULT LOCATION SCHEME FOR MEDIUM VOLTAGE DC SHIPBOARD POWER SYSTEM

Karthikeyan.M[a] , Rengaraj.R[b]

[a] Department of Electrical and Electronics Engineering, Velammal Engineering College, Chennai, India
[b] Department of Electrical and Electronics Engineering, SSN College of Engineering, Chennai, India
[a] Corresponding Author: M.Karthikeyan, E-Mail : karthik.keyan232@gmail.com, Tel: +919944100171

Abstract: *In this article, a fault location technique for medium voltage direct current (MVDC) shipboard power systems is presented. Accurate prediction of the fault location helps in restoration of the power in MVDC shipboard power systems. A portable device using probe power circuit (PPC) is used to estimate the location of the fault. The same circuit can be used to locate the fault in different zones of the MVDC shipboard power systems. The location of the fault is estimated using a non-iterative technique based on damping frequency and attenuation of the probe current. The proposed method using PPC is tested for fault close to PPC and different fault resistances. Test results indicate that the proposed method is simple, reliable, effective and accurate in locating the fault in MVDC shipboard power systems.*

Key words: *MVDC Shipboard power system, fault location, damping frequency, attenuation.*

1. Introduction

Medium voltage direct current zonal distribution architecture is proposed as a new distribution system for the all-electric ships in which the presence of power converters is pervasive [1]. These power electronic devices can significantly simplify the system by providing more available space, possible cost reduction, higher efficiency, higher safety, and variable control to achieve self-healing and survivability [2]. However locating the fault in MVDC shipboard power systems is a challenging task.

A traveling wave based fault locator is presented for accurate fault location on distributed overhead lines and underground cables [3]. Here, travelling time of the high-frequency voltage signal with a sampling rate of 200 MHz is used to determine the fault distance. However, the MVDC power system is of small scale, making it difficult to measure with enough accuracy the time difference. Furthermore, real effect, such as cable terminations, junctions and terminal connections may impact the performance of the method. Artificial neural network (ANN)–based fault classification and location in MVDC shipboard power system is presented in [4]. It is found to be efficient in detecting the type and location of dc cable faults. However, it needs large training sets and the learning process is consuming time. The apparent impedance calculated by using the fault voltage and current values is used to estimate the fault location [5]. A fault location method based on traveling wave is presented for multi-terminal DC (MTDC) system [6]. Fault distance is estimated using synchronized data with a communication infrastructure for the method presented in [7]. Active impedance estimation based fault location is presented for marine DC power system [8]. A fault location technique based on injection based method is presented for railway distribution system [9]. A fault location method using autoregressive modeling and extreme learning machine is presented for MVDC shipboard power system. But this method requires separate training for each zone [10].

A non-iterative fault location technique using PPC is presented for low voltage DC microgrid [11]. Fault distance is estimated without considering the damping coefficient of the probe current which leads to prominent error in fault location calculation. A non-iterative fault location technique including the attenuation constant in fault location calculation is presented for low voltage DC microgrid [12]. The restoration of power depends on the accurate fault location. For this purpose, a fault location method for MVDC shipboard power systems using probe power unit is presented in this paper. This portable PPC can be carried to the identified fault zone for fault location without installing it in every zone. The main objective of this work is to design a fault locator with accurate estimation of fault distance. This work also addresses the issue of fault close to PPC and high resistance faults. The rest of the paper is organized as follows. Section 2 gives a brief description about the MVDC shipboard architecture. Section 3 introduces the proposed fault location method. Section 4 presents the results and discussion. Finally section 5 contains the conclusion of the paper.

2. MVDC Shipboard architecture

Fig. 1 shows the MVDC ship board architecture. A port distribution bus and star distribution bus are the two buses that run longitudinally along the ship. The network is distributed as five zones. There are two generators G_1, G_2 that are connected to Zones 1 and 2 through power electronic converters and circuit breakers. Zone 3 and 4 supplies vital and non vital loads. Zone 5 consists of a radar load which is supplied from either of the MVDC buses through power electronic rectifier. The three types of fault that can occur in MVDC shipboard power system are (i) positive-rail-to-ground fault (PR–G), (ii) negative-rail-to-ground fault (NR–G) and (iii) rail-to-rail fault (R–R).

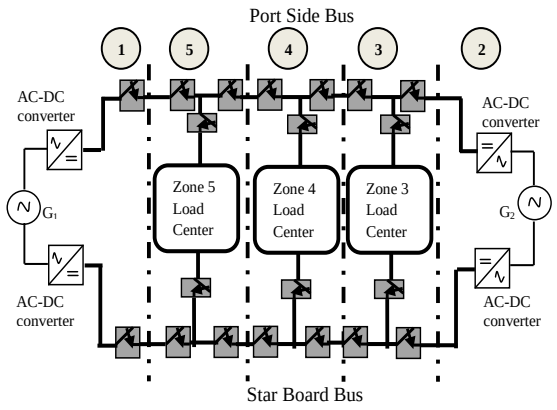

Fig.1. Architecture of MVDC shipboard power system

3. Proposed Fault Location Scheme

A MVDC shipboard power system is divided into five zones as shown in Fig.1. Once a fault is detected in any of the three zones (Zone 3, 4, and5), that particular zone is isolated without affecting the rest of the system. Once the faulted zone is identified, PPC needs to be switched on. The equivalent circuit for faulted zone with PPC is shown in Fig.2. The PPC consists of capacitor C_p, inductor L_p, a battery and switches. The capacitor is charged through battery and then discharged through the faulted path. Since the energy stored in C_p being finite, the probe current $i_p(t)$ decays over time. The fault location is estimated by using $i_p(t)$.

Once the fault zone is isolated, due to opening of S_1 and S_2, a loop consisting of RLC circuit is formed with PPC in the fault path as shown in Fig.2.

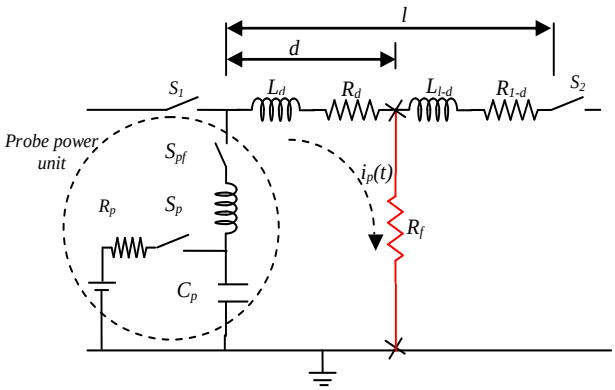

Fig.2. Equivalent circuit of faulted zone with PPC

The equation of the probe current for the circuit after closing the switches S_p and S_{pf} can be expressed as

$$\frac{d^2 i_p(t)}{dt^2} + \frac{R}{L}\frac{di_p(t)}{dt} + \frac{1}{LC} i_p(t) = 0 \qquad (1)$$

The equivalent resistance of the fault path will be given as the sum of the line and fault resistance. The equivalent inductance of the fault path will be given as the sum of the line and probe inductance (L_p) respectively. The line leakage capacitance can be neglected since the probe capacitance (C_p) is much larger than the line capacitance.

On solving (1), the probe current $i_p(t)$ can be written as,

$$i_p(t) = A_1 e^{-\alpha t} \cos(\omega_d t) + A_1 e^{-\alpha t} \sin(\omega_d t) \qquad (2)$$

Where ω_d and α are the damped frequency and attenuation of the probe current respectively. Constants A_1, A_2 can be found by using the initial conditions. For this circuit, the attenuation constant $\alpha = R/2L$.

Damping frequency and attenuation constant calculation

The probe current response is underdamped in the fault path and is shown in Fig.3. The damping frequency ω_d is extracted from the probe current by the method of averaging instead of FFT for reducing computation burden. $t_1, t_2 \ldots t_n$ are the instances at which the positive peaks of the probe current are $A_{t1}, A_{t2} \ldots A_{tn}$ respectively. The first six peaks of the probe current and the time instances at which it occurs are found from the probe current waveform. The damped frequency of probe current given by

$$\omega_d = \frac{\omega_{d1} + \omega_{d2} + \omega_{d3} + \omega_{d4} + \omega_{d5}}{5} \quad (3)$$

where, ω_{d1} is the frequency of the probe current between the time instances t_1 and t_2.

The attenuation constant α is found out by least square technique presented in [13]. Since the probe current response is exponentially decaying, the expression for the envelope of the probe current response can be written as

$$i_p env(t) = Ae^{-\alpha t} \quad (4)$$

Equation (4) can be written as

$$[A][x] = [m] \quad (5)$$

where,

$$[A] = \begin{bmatrix} 1 & -t_1 \\ 1 & -t_2 \\ 1 & -t_3 \\ 1 & -t_4 \\ 1 & -t_5 \end{bmatrix},$$

$$[m] = [A_{t1} \quad A_{t2} \quad A_{t3} \quad A_{t4} \quad A_{t5}]^T$$

$[x]$ is the column matrix of unknown $A, A\alpha$.

The unknown $[x]$ can be calculated from

$$[x] = [A]^+ [m] \quad (6)$$

where $[A]^+$ is the left pseudoinverse of $[A]$.

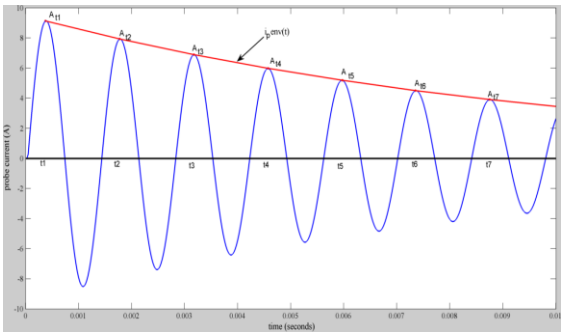

Fig.3. Probe current response: $t_1, t_2 .. t_7$ are the positive peak time instances and $A_{t1}, A_{t2} .. A_{t7}$ are the positive peak values.

Fault distance calculation

From the calculated damping frequency and attenuation constant, the natural frequency can be calculated as

$$\omega_n^2 = \omega_d^2 + \alpha^2 \quad (7)$$

Also, the natural frequency can be expressed in terms of the circuit components as

$$\omega_n = \frac{1}{\sqrt{(L_p + L_u d) C_p}} \quad (8)$$

From equation (7) & (8), the fault location d can be calculated as

$$d = \frac{1 - L_p(\omega_d^2 + \alpha^2) C_p}{L_u(\omega_d^2 + \alpha^2) C_p} \quad (9)$$

The % error can be calculated as

$$\% \text{ error} = \left| \frac{d_{cal} - d_{act}}{l} \right| \times 100 \quad (10)$$

where d_{cal} and d_{act} are the calculated and actual fault location respectively. l is the length of the MVDC line of the faulted zone.

Selection of Probe Capacitance and Inductance

The damping factor should be set to a low value to get a current oscillation from which enough information for fault location can be obtained. The capacitance and inductance ratio can be defined as a function of damping ratio and resistance.

$$\frac{C}{L} < \frac{4\varsigma^2}{R^2} = K. \quad (11)$$

For a full segment resistance of the MVDC line, the value of K is set as 0.01. The time taken by the probe current to decrease to 1A can be determined as

$$T_p = \frac{2L}{R} \ln\left(\sqrt{\frac{C}{L}} V_0\right) \quad (12)$$

The probe power unit inductance L_p and capacitance C_p can be determined for a probe period T_p as follows:

$$L_p = \frac{R}{2} \frac{T_p}{\ln\left(\sqrt{K} V_0\right)} - L_u l \quad (13)$$

$$C_p = (L_p + L_u l) K. \quad (14)$$

4. Results and Discussion

Simulation results have been obtained including different fault resistances and fault distances in the MVDC line using MATLAB. The developed MATLAB model is shown in Fig.4. The parameters of MVDC line and PPC are listed in Table I. For a damping factor of 0.025and 50-ms probing period T_p, the calculated probe power capacitance and inductance are 20.4μF and 1.742mH using (13) and (14). A rail-to-rail fault is simulated at a 1-km point with fault resistance 0.1 Ω. The probe current flowing through the fault path by the capacitor initial voltage of 100V is shown in Fig. 5. The probe current envelope obtained

by least square technique is shown in Fig. 6. The probe current decays as per the design and shows the oscillation frequency.

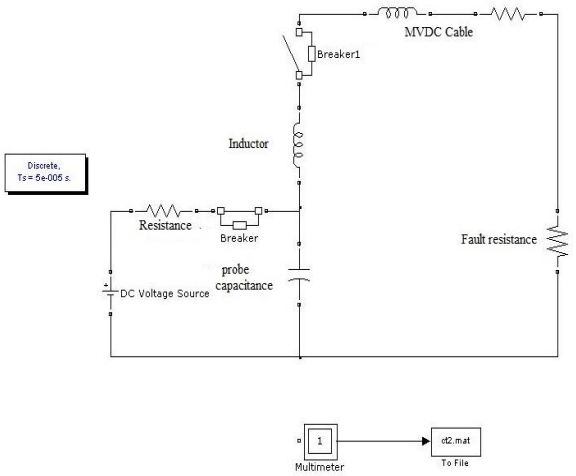

Fig.4. Simulink model of PPC

TABLE I
SIMULATION PARAMETERS OF MVDC LINE AND PPC

Resistance per km (R_u)	:	0.188 Ω/km
Inductance per km (L_u)	:	0.298893mH/km
Line length (l)	:	1 km
Fault location (d)	:	0-100%
Probe capacitance (C_p)	:	20.4μF
Probe inductance (L_p)	:	1.742mH
Capacitor initial voltage (V_p)	:	100 V
Fault resistance (R_f)	:	0-2 Ω

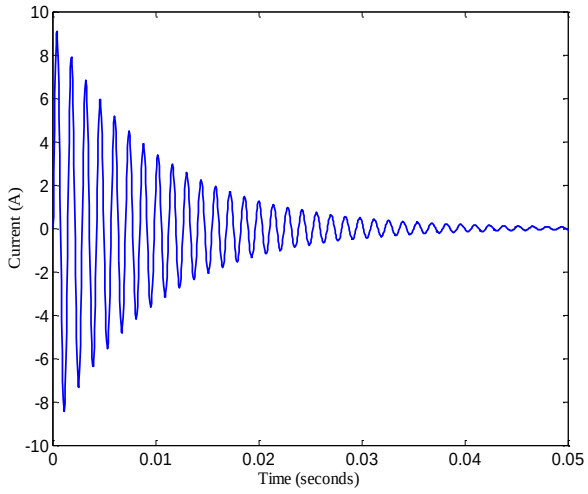

Fig.5. Probe current response

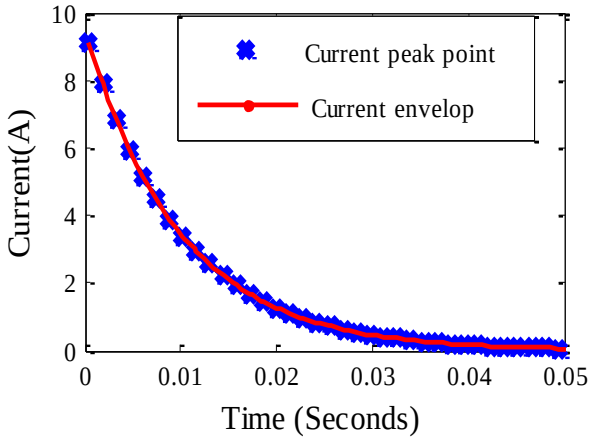

Fig.6. Probe current envelope

The damped frequency ω_d calculated from first six peaks of the probe current is 717.16 Hz for a sampling frequency of 40 kHz. Then by using the least square method, the attenuation constant is estimated. The calculated attenuation constant α is 141.61. The distance of the fault from the PPC is calculated by using (9) and % error is found to be 0.4613. The accuracy of the proposed method is tested with rail-to-rail fault and positive rail-to-ground fault. The robustness of the proposed method is tested with wide range of variables, such as fault position, fault resistance, sampling frequency. The fault distance varying from 10% to 100% of the faulted zone segment, 0.1 to 2.0Ω of fault resistance, 10 to 200 kHz of the sampling frequency have been used for testing the proposed fault location method. From Fig.7, it is inferred that the fault location % error is small unless the fault path is long (i.e towards the end of the faulted zone segment) with large fault resistance.

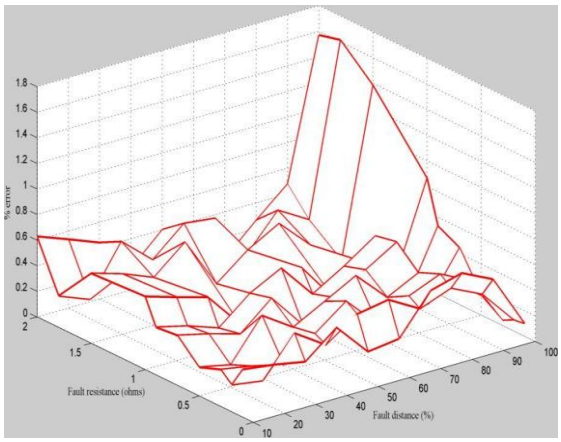

Fig.7. Fault location error for different fault distance and fault resistance

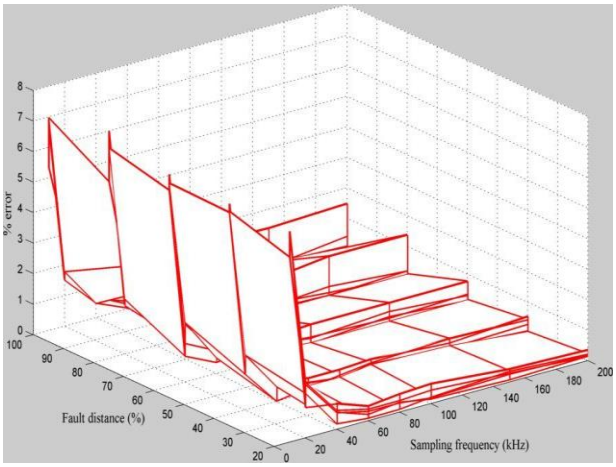

Fig.8. Fault location error for different sampling frequency and fault distance

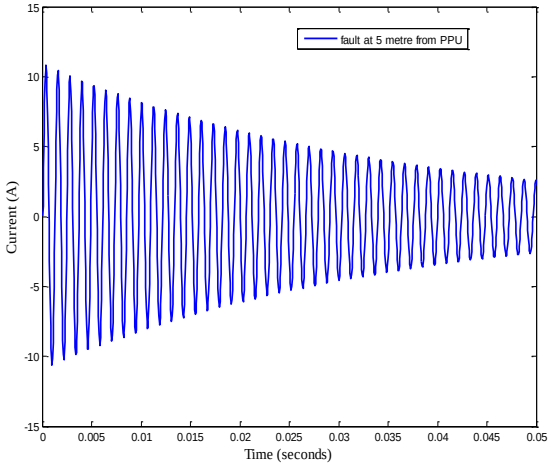

Fig.9. Probe current response for a fault close to PPC

The large fault resistance results in high value of the attenuation of probe current such that enough information cannot be obtained for accurate frequency estimation resulting in high % error. It is shown in Fig.8 that the % error can be maintained small with high sampling frequency. The minimum sampling frequency resulting in accurate fault location with less % error is 40 kHz. Hence a sampling frequency of 40 kHz is selected.

Performance of the proposed method for fault close to PPC

The performance of the proposed method is evaluated for a fault very close to PPC. A Rail-to-Rail fault is simulated at a distance of 5 m from PPC. The probe current response is shown in Fig.9. The damping frequency is calculated by (3) and it is found to be 830.1Hz for a sampling frequency of 40 kHz. Then, the attenuation constant α is calculated by least square technique and it is found to be 40.44. The distance of the fault from PPC is calculated using (9). The % error for this case is found to be 0.6078. The presence of significant damping does not affect the performance of the proposed method during a fault close to PPC. This is because of the $R, L, and\, C$ parameters of the MVDC line. Hence, a separate extra resistance circuit is not needed for the fault close to PPC as proposed in [12].

Hence the proposed method is not affected by fault close to PPC in MVDC shipboard power systems.

Performance of the proposed method for different fault resistances

The performance of the proposed method is studied for different fault resistances. The sampling frequency is kept as 40 kHz. Positive rail-to-ground fault and rail-to-rail fault are simulated with fault resistances from 0 to 2 ohms at different locations of the MVDC line. The damping frequency and attenuation are calculated. Then, the distance of the fault from PPC is calculated. The % error for various test cases is shown in Table II&III. From these tables, it is inferred that proposed method is not affected by high fault resistance. The % error for rail-to-rail fault is less than positive rail –to-ground fault. The maximum, minimum, mean, and standard deviations of % error are shown in Table IV. Also, expect three cases, the % error is found to be less than 1% for rail-to-rail fault. For positive rail-to-ground fault there are 16 test cases for which the % error is greater than 2.

These 16 test cases are analyzed and it is found that the estimated attenuation constant is less than the actual value. Considering the length of the MVDC line (1km), these % errors are within the acceptable limit. Hence the proposed method is suitable to locate the fault in MVDC shipboard power systems.

TABLE II
% ERROR FOR POSITIVE RAIL-TO-GROUND FAULT

d (%)	% error									
	R_f =0.1Ω	R_f =0.2Ω	R_f =0.3Ω	R_f =0.5Ω	R_f =0.7Ω	R_f =0.9Ω	R_f =1.0Ω	R_f =1.5Ω	R_f =1.8Ω	R_f =2.0Ω
10	0.8157	0.7002	1.8494	1.2275	1.6682	1.7849	1.6361	3.1979	1.4498	0.167
20	1.4844	1.3532	1.1625	1.953	0.9151	1.0398	2.2603	2.5295	2.0531	0.3983
30	1.0536	0.913	0.7203	1.4875	1.7667	0.4814	1.7988	2.1047	1.6447	0.0665
40	0.8466	0.6948	1.8934	1.2466	1.9237	2.0934	1.5319	1.9012	1.4318	0.3501
50	0.881	0.7236	1.9513	1.317	1.9082	2.3825	1.5202	1.8897	1.4108	0.3581
60	1.1529	0.9722	0.7419	1.4238	2.1579	1.1665	1.7555	2.1598	1.6666	0.1737
70	1.6794	1.4862	1.2223	1.9678	1.1052	1.6227	2.2143	2.6859	0.6381	1.2774
80	0.8931	0.682	1.9461	1.2976	1.8191	2.3465	1.3849	1.8759	1.337	0.6229
90	1.9154	1.7049	1.4264	2.2729	1.1738	1.7502	2.3465	2.8579	0.7358	1.2453
100	1.5578	1.3209	1.0362	1.8721	0.7558	1.3281	1.9167	2.5044	0.2995	1.7707

TABLE III
% ERROR FOR RAIL-TO-RAIL FAULT

d (%)	% error									
	R_f =0.1Ω	R_f =0.2Ω	R_f =0.3Ω	R_f =0.5Ω	R_f =0.7Ω	R_f =0.9Ω	R_f =1.0Ω	R_f =1.5Ω	R_f =1.8Ω	R_f =2.0Ω
10	0.3711	0.3383	0.2906	0.4883	0.2288	0.26	0.5651	0.6324	0.5133	0.0996
20	0.2116	0.1737	0.4734	0.3117	0.4809	0.5234	0.383	0.4753	0.3579	0.0875
30	0.2882	0.243	0.1855	0.356	0.5395	0.2916	0.4389	0.5399	0.4167	0.0434
40	0.2233	0.1705	0.4865	0.3244	0.4548	0.5866	0.3462	0.469	0.3342	0.1557
50	0.3895	0.3302	0.259	0.468	0.1889	0.332	0.4792	0.6261	0.0749	0.4427
60	0.3703	0.3097	0.2228	0.4244	0.5508	0.2781	0.4245	0.5915	0.019	0.5299
70	0.5706	0.4942	0.4249	0.1509	0.2677	0.4424	0.1398	0.3444	0.1636	0.861
80	0.5443	0.4691	0.3705	0.5778	0.1805	0.3742	0.5112	0.2722	0.0826	1.3805
90	0.246	0.1494	0.5282	0.3145	0.5288	0.4992	0.1454	0.4204	0.2754	1.6115
100	0.6272	0.5344	0.4384	0.1653	0.3986	0.3451	0.0324	0.2614	0.475	1.5672

TABLE IV
PERFORMANCE OF THE PROPOSED METHOD

Fault Type	Maximum error (%)	Minimum error (%)	Mean error (%)	Standard deviation
PR-G	3.1979	0.0665	1.4521	0.6323
R-R	1.6115	0.0190	0.3966	0.2556

To summarize, the proposed fault location technique consists of four steps. First, isolation of the faulted zone is to be done. Second, the damping frequency is calculated using the method of averaging after switching on the PPC. Third, the attenuation constant is calculated using least square method. Finally, the distance of the fault from the PPC is calculated using (9). The method locates the fault with less % error except few cases. The effect of fault resistance, fault distance and sampling frequency has been studied. The performance of the PPC is tested for fault close to PPC. The method is simple, effective and accurate as it does not use any communication or synchronized data.

6. Conclusion

A fault location technique for MVDC shipboard power systems is presented in this paper. The faulted zone is isolated and then portable PPC is used to locate the fault in the MVDC shipboard power systems. The components of the PPC are modeled as per the parameters of the MVDC shipboard power systems to generate an under damped probe current response. The probe current response is analyzed to calculate the distance of the fault from PPC. The method locates the fault with less % error except few cases and its performance is studied for variations in fault resistance, distance of fault, sampling frequency. The proposed method is simple, effective and accurate in locating the fault in MVDC shipboard power systems.

References

1. M. E. Baran and N. Maharajan. :*System reconfiguration on shipboard DC zonal electrical system*. In: Proceedings of IEEE, Electric Ship Technology Symposium., pp. 86-92, Jul.2005.
2. T. Ericsen, N. Hingorani, and Y. Khersonsky.: *Power electronics and future marine electrical systems.* In: IEEE Transactions on Industrial Appications., vol. 4, no. 1, pp. 155-163, Jan. 2006
3. Z. Q. Bo, G. Weller and M. A. Redfern.: *Accurate fault location technique for distribution system using fault-generated high-frequency transient voltage signals.* In: IEE Generation, Transmission and Distribution Proceedings, vol.146, no. 1, pp.73-79, Jan. 1999.
4. N. K. Chanda and Y. Fu.: *ANN-based fault classification and location in MVDC shipboard power systems*. In: Proceedings of North American Power Symposium, pp.1-7, Aug. 2011.merican
5. Girgis, A.A. Fallon, C.M. Lubkeman, D.L.*A fault location technique for rural distribution feeders*. In: IEEE Transactions on Industry Applications, vol.29, pp.2670-2676, 2009.
6. S.Azizi, M.Sanaya-Pasand, M.Abedini, and A.Hassani.: *A traveling wave-based methodology for wide area fault location in multiterminal dc systems*. In: IEEE Transactions on Power Delivery, vol. 29, pp.2552-2560, Dec 2014.
7. Y.H.Lin, C.W.Liu and C.S.Yu.: *A new fault locator for three terminal transmission lines using two-terminal synchronized voltage and current phasors*. In: IEEE Transactions on Power Delivery, vol. 17, pp.452-459, April 2002.
8. E.Christopher, M.Summer, and D.Thomas.: *Fault location in a zonal dc marine power system using active impedance estimation*. In : IEEE Transactions on Power Delivery, vol. 25, pp.860 -865, Mar. 2013.
9. H.Zhengyou, Z.Jun, L.Wei-hua, and L.Xiangning.: *Improved fault-location system for railway distribution system using superimposed signal*. In: IEEE Transactions on Power Delivery, vol. 25, pp.1899-1911, July 2010.
10. M.Karthikeyan, R.Rengaraj.: *Fault classification and location in MVDC Shipboard power systems using extreme learning machine.* In: Journal of Electrical Engineering, vol.17, no.1, pp. 427-438, ISSN: 1582-4594
11. J.D.Park, J.Candelaria, L.Ma, and K.Dunn.: *DC ring-bus microgrid fault protection and identification of fault location*. In: IEEE Transactions on Power Delivery, vol. 28, no.4, pp.2574-2584, october 2013.
12. Rabindra Mohanty, U.Sri Mukha Balaji, and A.K.Pradhan.: *An accurate non-iterative fault location technique for low voltage DC microgrid*. In: IEEE Transactions on Power Delivery, vol. 31. no.2 pp.475-481, April 2016.
13. M.Sachdev and M.Nagpal.: *A recursive least error square algorithm for power system relaying and measurement applications.* In: IEEE Transactions on Power Delivery, vol. 6. pp.1008-1015, July 1991.